10.2478/v10170-011-0041-z

Archives of Control Sciences
Volume 23(LIX), 2013
No. 1, *pages 41–59*

Robust control of depth of anesthesia based on H_∞ design

DANIELA V. CAIADO, JOÃO M. LEMOS and BERTINHO A. COSTA

This paper presents a case study on the design of a robust controller for the depth of anesthesia (DoA) induced by the drug *propofol*. This process is represented by a linear model together with a non-parametric uncertainty description that is evaluated using a patient model bank with 20 patients undergoing sedation. By using H_∞ methods, the controller is aimed to comply with robust stability and performance specifications for the class of patient models considered. A minimization problem of sensitivity and complementary sensitivity is made to design the controller. The controller that results from this procedure is approximated by a controller with a lower order, that in turn is redesigned in discrete time for computer control application. The resulting controller is evaluated in simulations using a realistic nonlinear model of DoA.

Key words: depth of anesthesia, model uncertainty, robust control feedback, H_∞ design, μ-synthesis

1. Introduction

1.1. Framework

The drug administration for anesthesia in a surgical procedure is not a straightforward process that is based on guidelines, with respect to the patients physiological characteristics, and on the anesthetist past experience, besides it is time consuming.

The drug absorption, distribution, metabolism and elimination on a single patient is unique and varies with time, being the source of inter- and intra-patient variability and turning the task of the anesthetist very difficult to perform.

In general anesthesia, three targets are aimed: muscular paralysis for intubation and proper surgical intervention, absence of pain and hypnosis or depth of anesthesia (DoA) for the patient's well-being. Each target is reached with the administration of different drugs. For the case of DoA, sedative drugs, like *propofol*, are administered for the patient

D.V. Caiado is with INESC-ID, Lisboa, Portugal, e-mail: danielavcaiado@gmail.com. J.M. Lemos and B.A. Costa are with INESC-ID/IST, Lisboa, Portugal, e-mails: jlml@inesc-id.pt, bac@inesc-id.pt.

This work has been performed in the framework of project *GALENO - Modeling and control for personalized drug administration*, supported by Fundação de Ciência e Tecnologia, Portugal, under contract PTDC/SAU-BEB/103667/2008, and PEst - OE/EEI/LA0021/2011.

Received 11.02.2013.

to reach an adequate level of hypnosis. For this kind of drugs, side-effects resulting from under- or over-dosing are existent, for instance the possibility of postoperative morbidity or even mortality as a result of over-dosing, on the other way, the under-dosing that results in the patient awareness during the surgery may be harmful and may result in psychological trauma.

Accurate drug delivery may be possible to obtain with automatic control systems, improving current actual clinical practice and liberating the anesthetist to concentrate on important issues that relate the patients state. Although there are automatic control systems already is use, the majority of the procedures is still performed with discontinuous *bolus* infusions, in an open-loop feedback system. For DoA, the level is inferred from several physiological reactions, such as the loss of eye lash reflex. Recently, the measurable BIS index [12], a measure of the electroencephalogram signal that assesses brain wave activity to determine the level of hypnosis, provides a way to automatic feedback control for DoA together with sedative drugs, such as *propofol*.

The use of this kind of technologies may reduce under- or over-dose risks, the total amount of drug infused and the anesthetist workload.

1.2. Literature review

Pharmacokinetic (PK) and pharmacodynamic (PD) models for the patient response to *propofol* have been developed [10, 15, 6] based on a multi-compartmental structure, with equilibrium constants that relate the drug mass migration between compartments. The PD model for sedatives comprises a nonlinear term [8], that relates the drug concentration in the body with the actual effect, measured by the BIS index. The administration of analgesic drugs, such as *remifentanil*, has been shown to interfere on the BIS index and to have a synergic interaction in the sedation effect of *popofol* [4].

The automatic drug delivery of sedatives based on the BIS index, as the measured variable, has been addressed using several control strategies. Fixed-gain proportional-integrative-derivative (PID) controllers have been developed and have provided adequate performances in the clinical environment [13, 1, 9]. Other strategies, such as model predictive control (MPC) [14], neural network based control [11] or fuzzy logic control [16], among others, have been applied for *propofol* delivery control systems.

With some surprise, due to the high levels of uncertainty involved in modeling patients behavior, in the field of anesthetics administration, robust control strategies have been rarely applied. PID control, CRONE control [5], internal model control (IMC) [2] or predictive control [7] are the few kinds of algorithms applied to this subject with robust control techniques.

1.3. Paper contributions and organization

The variability in the patients response is related to many aspects such as age, gender, health status, or even total drug uptake or time. The variability between patient models is referred to as model uncertainty and is the major issue taken into account in this paper. Controller design in the presence of these uncertainties is approached with robust

control techniques, with performance and stability specifications. In a feedback control framework, the controller is designed to deliver an adequate performance on drug administration and to be able to stabilize the class of patient models. The design problem is approached with the H_∞ control theory, imposing specifications on reference tracking, output disturbances and noise rejection. The contribution of the paper consists thus of a methodology of robust controller design for DoA and its demonstration on simulation on a realistic nonlinear model, with uncertainty characterized from patient clinical data.

The paper is organized as follows: the mathematical model that describes the patient response as a function of the drug dose input is presented in section 2, followed by the description of the control design algorithm, in section 3; robust performance and stability requirements are checked in section 4 and the conclusions are drawn in section 5.

2. Mathematical model

The PK/PD model used in this work is described in this section. Whereas the pharmacodynamics (PD) refers to the actual effect of the drug in the patient, as a function of its concentration, the pharmacokinetics (PK) describes the drug concentration in the tissues as a function of time and drug dose.

2.1. Pharmacokinetics

The pharmacokinetic part of the model is assumed to be described by three compartments as represented in Fig. 1. First, the drug enters the body in the central compartment (blood, liver and brain), where the drug metabolism and elimination occurs. This compartment is connected with two other peripheral compartments, with distinct equilibrating rates: a fast equilibrating compartment (2 in Fig. 1), that represents the distribution of the central nervous system (CNS) to the muscles and organs, and the slow equilibrating compartment (3 in Fig. 1), that represents the drug distribution in the bones and fat tissue, with distinctly slower constant rates.

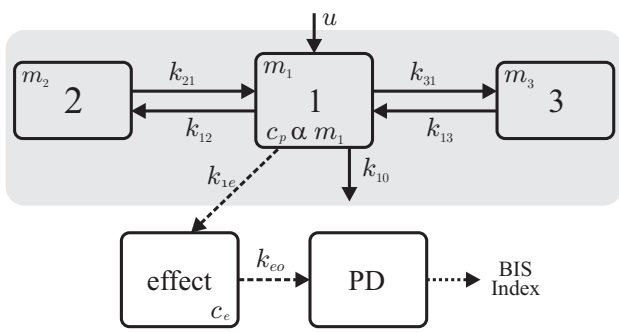

Figure 1. Schematic representation of the compartmental model for the dynamic response of hypnosis. The shadowed region is the PK part of the model.

The PK compartmental model, that relates the drug infusion u (ml/h) with the drug plasma concentration c_p (μg/ml), can be described in the state-space form,

$$\begin{bmatrix} \dot{m}_1 \\ \dot{m}_2 \\ \dot{m}_3 \end{bmatrix} = \begin{bmatrix} -(k_{10}+k_{12}+k_{13}) & k_{21} & k_{31} \\ k_{12} & -k_{21} & 0 \\ k_{13} & 0 & -k_{31} \end{bmatrix} \begin{bmatrix} m_1 \\ m_2 \\ m_3 \end{bmatrix} + \begin{bmatrix} \frac{10000}{3600} \\ 0 \\ 0 \end{bmatrix} u \tag{1}$$

$$c_p = \begin{bmatrix} \frac{1}{1000 \times V_1} & 0 & 0 \end{bmatrix} \begin{bmatrix} m_1 \\ m_2 \\ m_3 \end{bmatrix}, \tag{2}$$

where m_i (μg), with $i = 1,2,3$, is the mass in the compartment i, k_{ij} (s^{-1}), with $i,j = 1,2,3$, is the equilibrium constant from the i-th to the j-th compartment and V_1 (l) is the volume of the central compartment. The irreversible elimination or biotransformation of the drug is described by k_{10}.

2.2. Pharmacodynamics

An extra compartment can be added to the PK model, representing the transition from the drug plasma concentration to the drug effect concentration c_e. This is a first term of the PD model that is linear and is described by

$$\dot{c_e} = -k_{eo}c_e + k_{1e}c_p, \tag{3}$$

where k_{1e} (s^{-1}) is the equilibrium constant between the central and the effect-site compartments and is considered to be equal to k_{eo} (s^{-1}), that is the equilibrium constant from the effect-site compartment to a hypothetical compartment where the effect is measured and the drug leaves the body.

The drug effect observed on the patient is expressed as a nonlinear function of the effect-site concentration, by

$$BIS = E_0 + (E_{max} - E_0)\frac{c_e^{\gamma}}{c_e^{\gamma} + C_{50}^{\gamma}}, \tag{4}$$

where E_0 is the baseline effect at zero concentrations, E_{max} is the peak of the drug effect, C_{50} is the concentration that yields 50 % of the maximum drug effect and γ is the steepness of the concentration-response relation.

The analgesic drug has an effect that must also be taken into account in the model. Moreover, the two kinds of drug (hypnotic and analgesic) act in a synergic way. In this case, the hypnotic drug considered is *propofol*, whereas the analgesic drug considered is *remifentanil*. To distinguish the variables associated with the hypnotic model from the variables associated with the analgesic models, the super-indexs *prop* and *remi*, respectively, are added to the symbols that denote the different variables. Therefore, c_e^{prop} denotes the concentration in the effect-site compartment of *propofol*, and c_e^{remi}denotes the

concentration in the effect-site compartment of *remifentanil*. The existing correlation between the effect of analgesic drugs, such as *remifentanil*, and the effect of hypnotic drugs, in this case *propofol*, is expressed in the overall effect as

$$BIS = \frac{E_0}{1 + \left(U^{prop} + U^{remi}\right)^{\gamma}}, \tag{5}$$

where U^{prop} and U^{remi} are the normalized effect-site concentrations defined as

$$U^{prop} = \frac{c_e^{prop}}{C_{50}^{prop}}, \qquad U^{remi} = \frac{c_e^{remi}}{C_{50}^{remi}}. \tag{6}$$

2.3. Linear PK/PD model

The PK model (1,2) and the the fist term of the PD model (3), may be described by the state-space model

$$\begin{cases} \dot{x}(t) = \Phi\, x(t) + \Gamma\, u(t) \\ c_e(t) = \mathbb{I}\, x(t), \end{cases} \tag{7}$$

where Φ is a matrix with patient dependent parameters given by

$$\Phi = \begin{bmatrix} -(k_{10} + k_{12} + k_{13}) & k_{21} & k_{31} & 0 \\ k_{12} & -k_{21} & 0 & 0 \\ k_{13} & 0 & -k_{31} & 0 \\ \frac{k_{eo}}{1000 \times V_1} & 0 & 0 & -k_{eo} \end{bmatrix}, \tag{8}$$

x is the state and Γ contains a factor for unit conversion of the drug dose, such as

$$x = \begin{bmatrix} m_1 \\ m_2 \\ m_3 \\ c_e \end{bmatrix}, \quad \Gamma = \begin{bmatrix} \frac{10000}{3600} \\ 0 \\ 0 \\ 0 \end{bmatrix}, \quad \mathbb{I} = \begin{bmatrix} 0 & 0 & 0 & 1 \end{bmatrix}, \tag{9}$$

and t is the continuous time measured in seconds.

The state-space system (7) is expressed, in the Laplace transform domain, by

$$c_e(s) = F(s)\, u(s), \tag{10}$$

where $F(s)$ is the transfer function of the linear part of the model and s is the Laplace variable.

The linear approximation of the nonlinear description of the observed effect as a function of the effect-site concentration (5) is accomplished by Jacobian linearization at an equilibrium point. This term affects only the static gain of the linear part of the model

and is patient dependent. From (5), at the equilibrium value of $\overline{BIS}$, the equilibrium value of the effect-site concentration $\overline{c_e^{prop}}$ is

$$\overline{c_e^{prop}} = \left[\sqrt[\gamma]{\frac{E_0}{\overline{BIS}} - 1} - U^{remi} \right] C_{50}^{prop}. \tag{11}$$

The BIS derivative with respect to the increments of the effect-site concentration, η, is given by

$$\eta = \frac{\partial}{\partial c_e^{prop}} BIS \Big|_{c_e^{prop} = \overline{c_e^{prop}}} = \frac{E_0\, \gamma}{C_{50}^{prop}} \frac{\left(\frac{\overline{c_e^{prop}}}{C_{50}^{prop}} + U^{remi} \right)^{\gamma - 1}}{\left[1 + \left(\frac{\overline{c_e^{prop}}}{C_{50}^{prop}} + U^{remi} \right)^{\gamma} \right]^2}, \tag{12}$$

and represents the static gain of the nonlinear term of the model, that relates the increment of the drug effect-site concentration with its effect given by the increment of the BIS index with respect to its equilibrium value. In this case study, the *remifentanil* dose appears in the model as a disturbance.

From (12) and (10) the linearized model, ignoring the effect of the analgesic drug, is described by

$$BIS(s) = G(s)\, u(s), \tag{13}$$

where $G(s)$, with $G(s) = F(s)\, \eta$, is the transfer function that relates the patient response, measured by the BIS index, with the drug dose.

3. Controller design

Clinically, the level of the depth of anesthesia at which the patient should be kept at is 50, and should never be lower than 30. In this case, a feedback control system that compares the reference value, that is 50, with the measured value of the BIS index, at each instant, is considered. As shown in Fig. 2, the controller (K) compares the value of the BIS index (y) with the desired level (r), and computes the amount of drug (u) that is required to deliver to the patient (G) in order to attain the desired level. Accordingly, the manipulated variable is the increment of the drug dose u and the measured variable is the BIS index y, that is affected by the sum of all disturbances d acting on the system and by the sensor noise signal n. Such a system is described by the closed-loop model

$$y = \frac{1}{1+KG}\, d + \frac{KG}{1+KG}\, r - \frac{KG}{1+KG}\, n. \tag{14}$$

The transfer function from d to y is the sensitivity function, $S(s)$, and the transfer function from r to y is the complementary sensitivity function, $T(s)$. The transfer function $n \to y$ is $-T(s)$

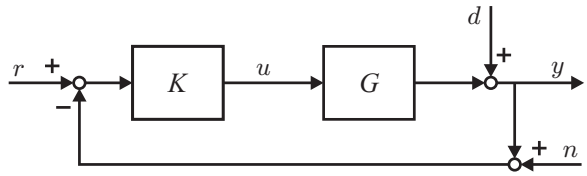

Figure 2. Schematic representation of the control system.

In this case, the drug is administered to the patient through a syringe that is commanded by a computer that runs the controller algorithm, sampling the BIS index value every 5 seconds.

In this paper, an approach of the H_∞ optimal control design technique [17] is used to design an adequate controller for the problem at hand. The goal is to obtain a controller able to provide robust performance and robust stability, in the presence of model uncertainty, load disturbances and sensor noise. This controller is designed based on a class of 20 models, $\mathcal{G} = \{G_i,\ i = 1,2,...,20\}$, obtained from patients subject to sedation. Under these circumstances, input disturbance rejection and high frequency sensor noise rejection are problems to take into account in the control design, as well as the problem of zero steady-state tracking error, that is accomplished with the inclusion of an integral term.

3.1. Robust stability

The stability of the controlled system is the main goal in this work and, though performance is very important, one has to ensure that the patient DoA is stabilized by the controller. Therefore, for robust stability, the goal is to synthesize a stabilizing controller for all the models in the given class, $\mathcal{G} = \{G_i,\ i = 1,2,...,20\}$, referred as *patient model bank*. For this sake, it is assumed that the true model $G(s)$ of a given patient can be written as a function of a nominal model $G_N(s)$ as

$$G(j\omega) = G_N(j\omega)(1+\Delta(j\omega)), \tag{15}$$

where Δ is the multiplicative uncertainty at frequency ω.

In Fig. 3, the frequency response of the models G_i shows that there is a wide range of dynamic behaviors within these models. This high variability in the dynamic behaviors is a major difficulty in the design of a suitable controller for all the models. To obtain the best possible controller in terms of performance, two models are not used for controller design (models G_4 and G_{14}), being treated separately.

From the Nyquist stability criterion, it can be inferred that the controller K, that is designed to stabilize the nominal model G_N, also stabilizes G if the following robust stability condition holds

$$|KG_N(j\omega) - KG(j\omega)| < |1 + KG_N(j\omega)|. \tag{16}$$

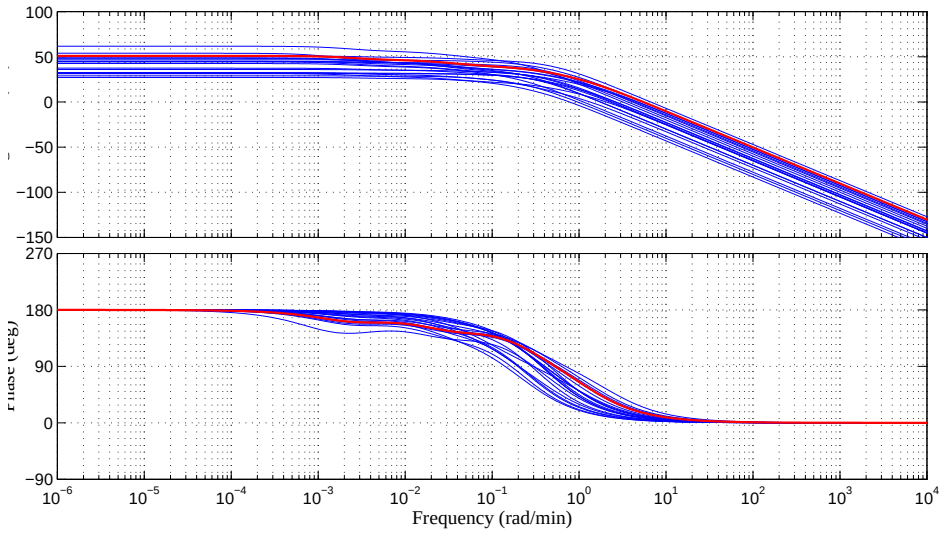

Figure 3. Frequency response of all the $G(s)$ models in the patient bank. The nominal model is represented in red.

With (15), condition (16) can be written in the form

$$|\Delta(j\omega)| < \frac{|1+KG_N(j\omega)|}{|KG_N(j\omega)|}. \tag{17}$$

Let $l(\omega)$ be an upper bound function of the multiplicative uncertainty, meaning that

$$|\Delta(j\omega)| = \frac{|KG_N(j\omega)-KG(j\omega)|}{|KG_N(j\omega)|} < l(\omega). \tag{18}$$

If $l(\omega)$ is such that

$$l(\omega) < \frac{|1+KG_N(j\omega)|}{|KG_N(j\omega)|}, \tag{19}$$

condition (16) is thus satisfied, and all the models that verify (19) will be stabilized by the controller K.

Condition (19) may be written in the form

$$\frac{1}{l(\omega)} > \frac{|KG_N(j\omega)|}{|1+KG_N(j\omega)|} = |T_N(j\omega)|, \tag{20}$$

where T_N is the complementary sensitivity function of the nominal model coupled with the controller and corresponds to the closed-loop transfer function. Therefore, if an upper bound function $l(\omega)$ for the multiplicative uncertainties exists such that its inverse is also an upper bound for the complementary sensitivity function, the controller designed for the nominal model has robust stability, meaning that all the systems G_i that satisfy (19) are stabilized by the nominal controller.

3.2. Robust performance

In terms of performance, the controller is expected to be robust, being designed to reject load disturbances and high frequency sensor noise, in the presence of model uncertainty.

Following [17], the load disturbance rejection objective is defined as a weighted sensitivity minimization problem and the measurement noise rejection objective is defined as a weighted complementary sensitivity minimization problem. These two goals are closely related through the specification of the controlled system bandwidth (by the sensitivity function) and reference tracking and robust stability specifications (related to the complementary sensitivity function).

In order to tackle the above minimization problems, two weighting functions are incorporated in the system, as depicted in Fig. 4. In this case, W_S and W_T affect the

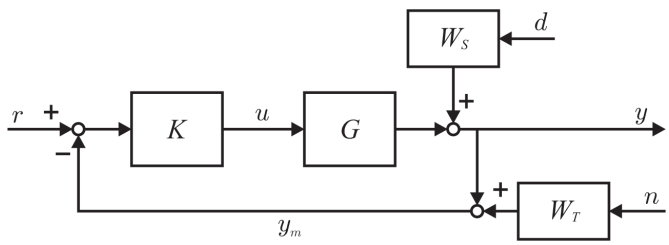

Figure 4. Schematic representation of the control action with the weighting functions.

sensitivity and the complementary sensitivity functions, respectively, and the closed-loop system is

$$y = \frac{1}{1+KG} W_S\, d + \frac{KG}{1+KG}\, r - \frac{KG}{1+KG}\, W_T\, n. \tag{21}$$

Since, for performance purposes of rejecting load disturbances, the gain of the weighted sensitivity function must be kept below 1, then it must be

$$|S \times W_S| < 1 \qquad \Leftrightarrow \qquad |S| < \frac{1}{|W_S|}, \tag{22}$$

where S is the sensitivity function given by

$$S = \frac{1}{1+KG}. \tag{23}$$

This weighted sensitivity function enforces the desired bandwidth while the weighted complementary sensitivity function enforces the adequate roll-off outside the bandwidth in which the disturbances are rejected.

The noise rejection problem is approached in the same way, as the gain of the weighted complementary sensitivity function must be kept below 1, so that

$$|T \times W_T| < 1 \qquad \Leftrightarrow \qquad |T| < \frac{1}{|W_T|}, \tag{24}$$

where T is the complementary sensitivity function given by

$$T = \frac{KG}{1+KG}. \tag{25}$$

Conditions (22) and (24) must be satisfied for each S_i and T_i, with $i = 1,...,20$, of all G_i models. This is achieved by selecting W_S and W_T to have the frequency response shown in Fig. 5.

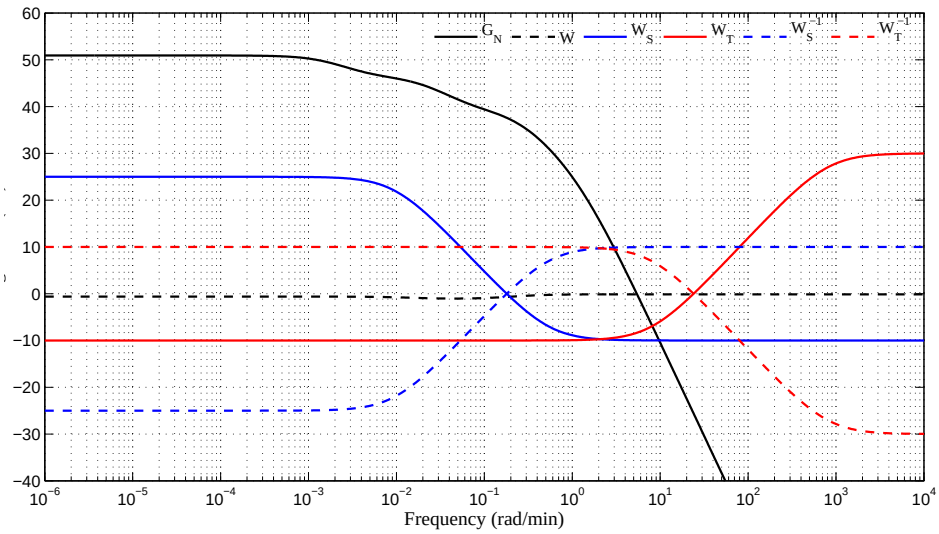

Figure 5. Magnitude of the weighting functions W_S and W_T and of the respective inverse functions W_S^{-1} and W_T^{-1}. The nominal model G_N and the cover (upper bound function) of all uncertainties W are also shown.

The weight W_T^{-1} is a low-pass function whose shape is selected such as to ensure reference tracking up to the desired bandwidth (that implies that W_T^{-1} is small) and noise rejection in the higher frequency band, as well as robustness with respect to high frequency model uncertainty (that implies that W_T^{-1} is big in this band). A dual behavior follows to W_S^{-1}.

The controller is also designed with integral action in order to overcome possible steady-state errors.

4. Controller analysis

With all the performance and robust stability specification taken into account, the controller synthesis is performed by using the DK algorithm for μ-synthesis [17], in the implementation provided by the function `dksyn` of MATLAB®, described by *Robust Control Toolbox* ™ User's Guide [3].

The controller takes the form of a state-space model and is designed for the nominal model G_{15}, with the W_S and W_T of Fig. 5, being described by

$$\begin{cases} \dot{x_c}(t) = A\, x_c(t) + B\, e(t) \\ u(t) = C\, x_c(t), \end{cases} \tag{26}$$

where A, B and C are the matrices that result from the design algorithm, e is the tracking error, $e = r - y_m$, and x_c is the controller state.

4.1. Stability analysis

Closed-loop stability can be checked by analyzing the loop-gain frequency response. Therefore, the closed-loop is stable if

$$|KG(j\omega)| < 1 \quad \text{at the frequency } \omega \text{ for which} \quad \angle KG(j\omega) = -180^\circ. \tag{27}$$

The loop-gain response of all models of the patient model bank is shown in Fig. 6, where the stability condition is proved to be fulfilled.

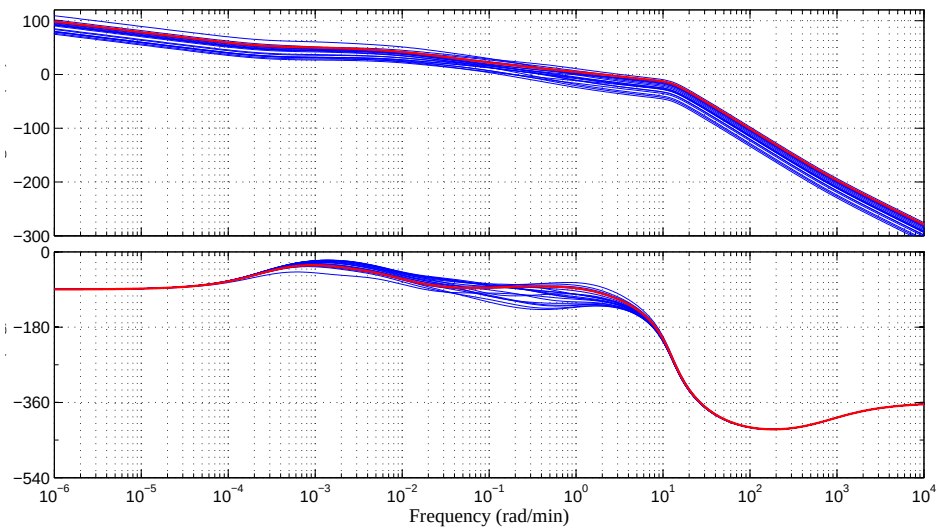

Figure 6. Loop-gain frequency response. The nominal model is represented in red.

To verify if the controller is able to stabilize all the models, one has to check the existence of an upper bound function $l(\omega)$ that yields conditions (19) and (20). These conditions are proved to be verified for the function $l(\omega) = (0.98s+0.010)/(s+0.0106)$, in Fig. 7 and Fig. 8. The frequency responses of $l(\omega)$, in Fig. 7, and of $l^{-1}(\omega)$, in Fig. 8, show that this controller is robustly stable except for the models excluded from the design (G_4 and G_{14}).

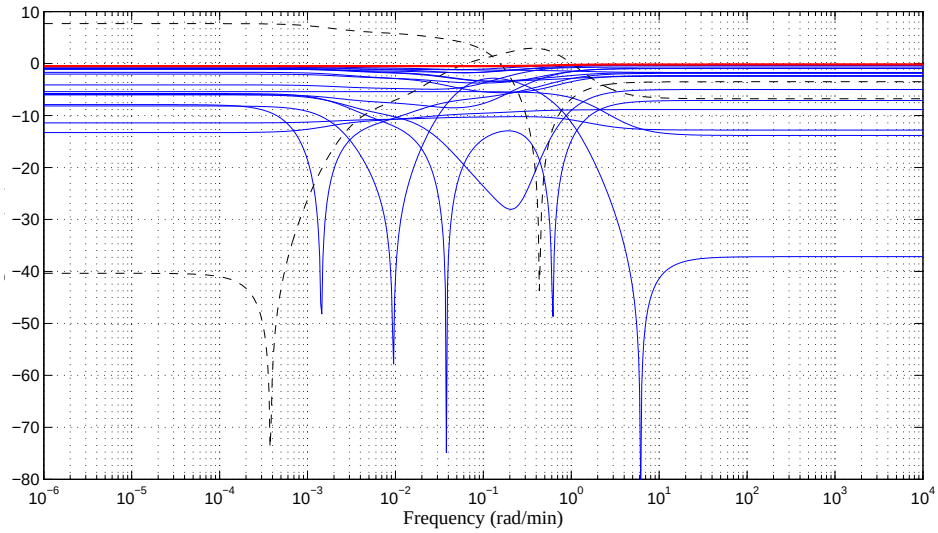

Figure 7. Magnitude of the multiplicative uncertainty Δ of the loop-gain. The function $l(\omega)$ is represented in red. The dashed black lines represent the uncertainty of models G_4 and G_{14} (that are excluded from the design).

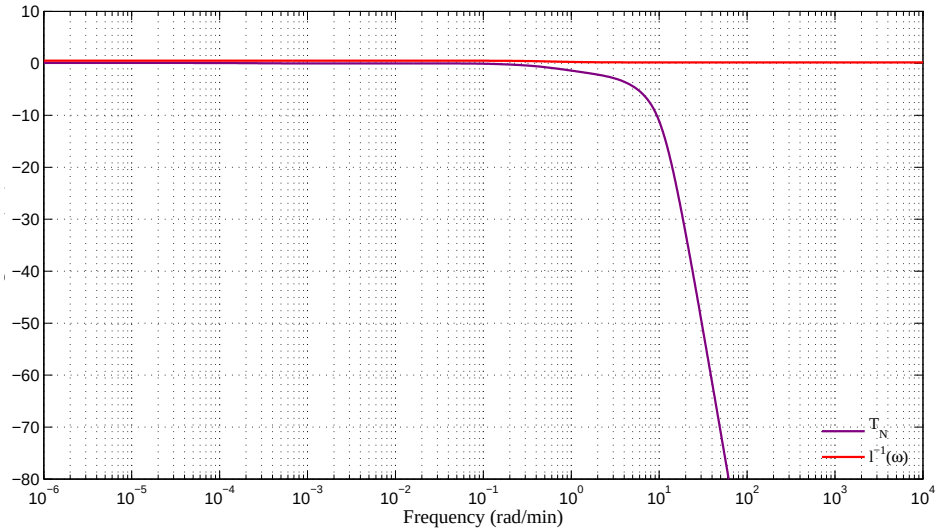

Figure 8. Gain of the inverse upper bound function for multiplicative uncertainty $l^{-1}(\omega)$ and the nominal complementary sensitivity function T_N. This plot is used to verify the robust stability condition.

4.2. Performance analysis

The performance specifications imposed for the controller design are now checked. The performance condition described as weighted sensitivity minimization problem and

defined in condition (22) is fulfilled for all the models except for model G_2, as shown in Fig. 9. The results of the weighted complementary sensitivity minimization problem are

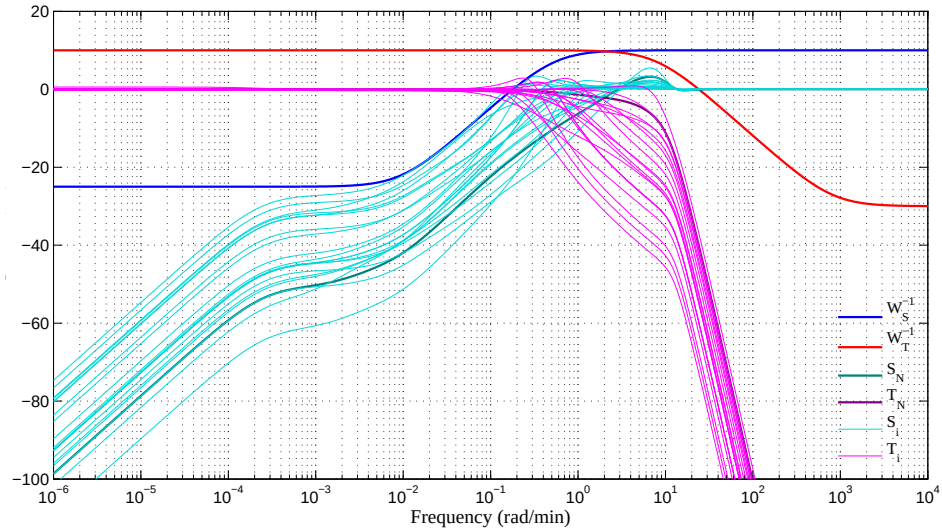

Figure 9. Gain of the sensitivity functions S and the complementary sensitivity functions T , with the upper bounds W_S^{-1} and W_T^{-1}.

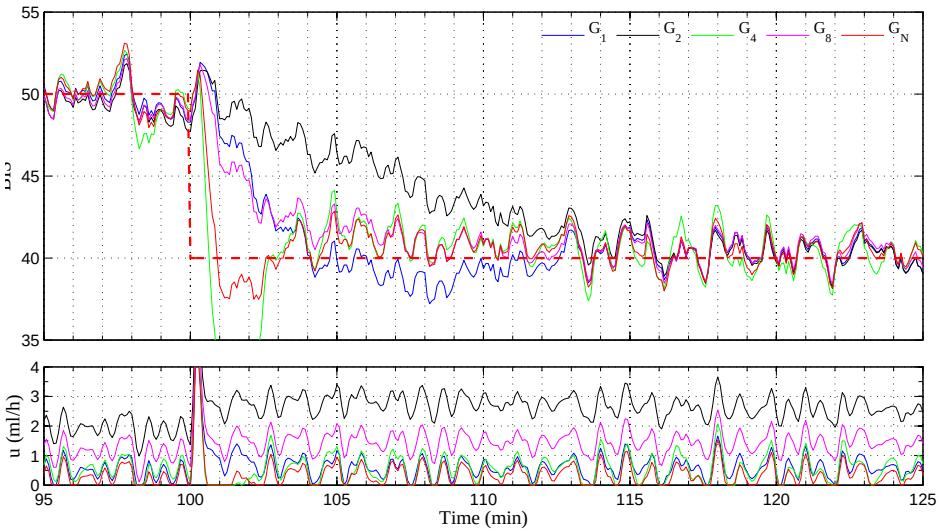

Figure 10. Time response of the controlled systems and the control action (u) for 5 models (G_1, G_2, G_4, G_8 and G_N). Simulations are performed in the presence of a noise signal similar to the real noise. At 100 min, a step of -10 is performed. The reference is represented by the red dashed line.

also shown in Fig. 9, where condition (24) is met for all the models, since the functions T_i, with $i = 1, ..., 20$, fall below the bound function W_T^{-1}.

The time response to a step reference of 5 random models, in continuous time, is depicted in Fig. 10 showing that the controller provides an adequate control action in order to maintain the patient model at the desired level of DoA.

In spite of the controller not being able to *a priori* guarantee stability for models G_4 and G_{14}, the time response of the controller with model G_4 (Fig. 10) shows that the controller is able to provide an acceptable performance. A similar situation holds for G_{14}

4.3. Computer application

For computer application, the 21st– order controller that directly results from the μ-synthesis design procedures is approximated by a lower order of 5. The order reduction is performed without the integral term for which the controller of order 20 is reduced to a 4th– order. As shown by the Hankel singular value plot of the controller state-space representation, depicted in Fig. 11, the majority of the system modes is well preserved in the 4th– order controller. The integral action is then added.

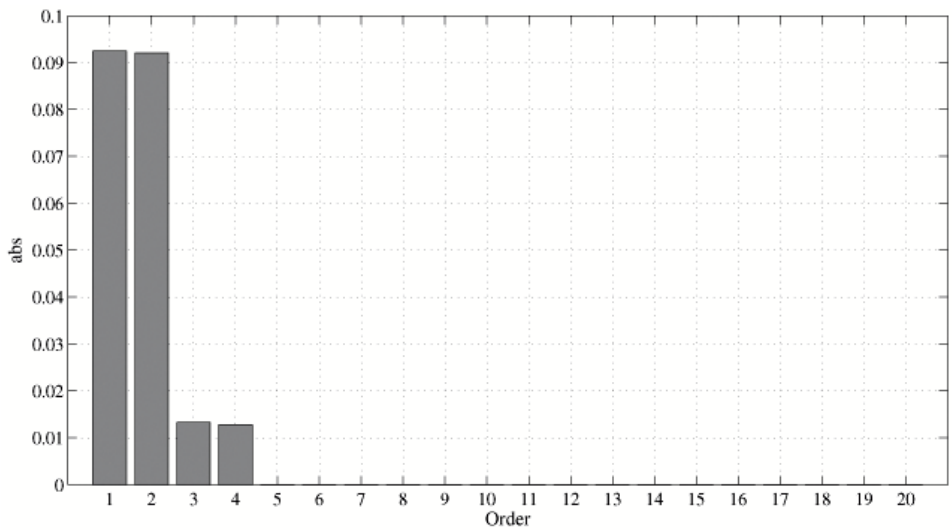

Figure 11. Hankel singular value plot for the controller order reduction.

To prove that this order reduction is adequate, the loop-gain frequency response of the nominal model is compared with the full order controller, in Fig. 12.

The sensitivity function and the complementary sensitivity function of the reduced-order controller are also compared in Fig. 13 with the ones of the full order controller. This comparison shows a very good agreement between both controllers in the frequency range of interest. This fact, as well as the agreement of time response, shown in Fig. 14, justifies the use of the reduced complexity controller.

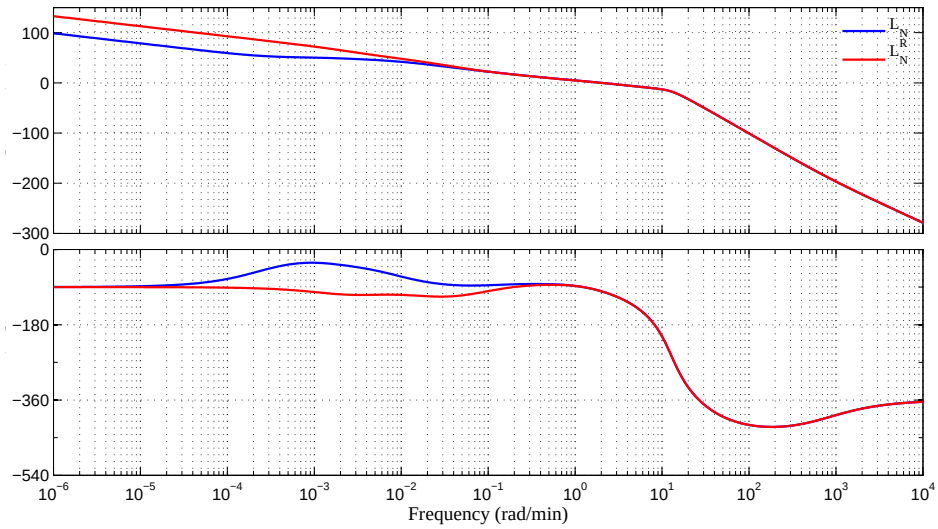

Figure 12. Loop-gain frequency response of the controlled nominal model with the full order controller and with the reduced-order controller (L_N^R).

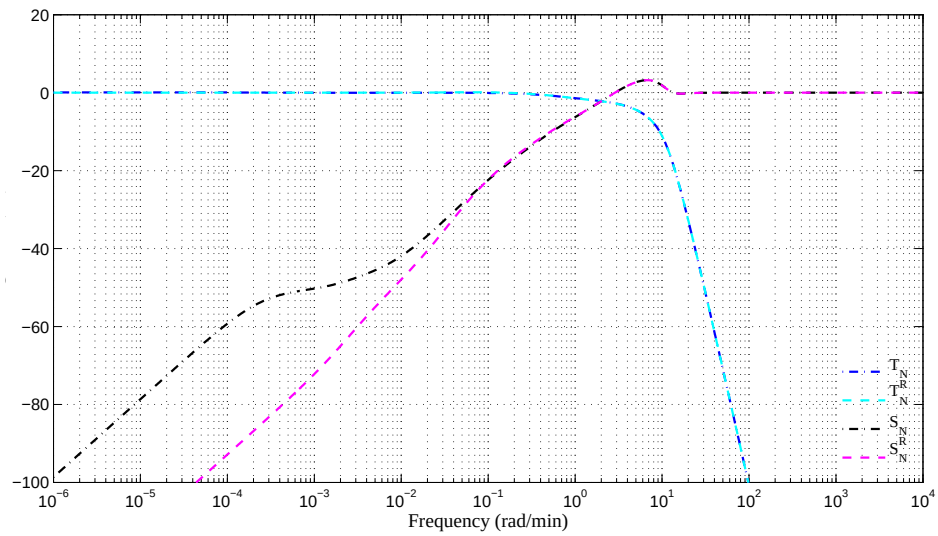

Figure 13. Gain of the sensitivity and complementary sensitivity functions of the controlled nominal model with the full order controller and the reduced-order controller (S_N^R, T_N^R).

The use of an order between 5 and 21 does not bring noticeable improvements in either frequency and time responses (data not shown).

The reduced order controller, designed in continuous time, is discretized with the zero-order hold method, with a sampling time of 5 seconds. The loop-gain with the

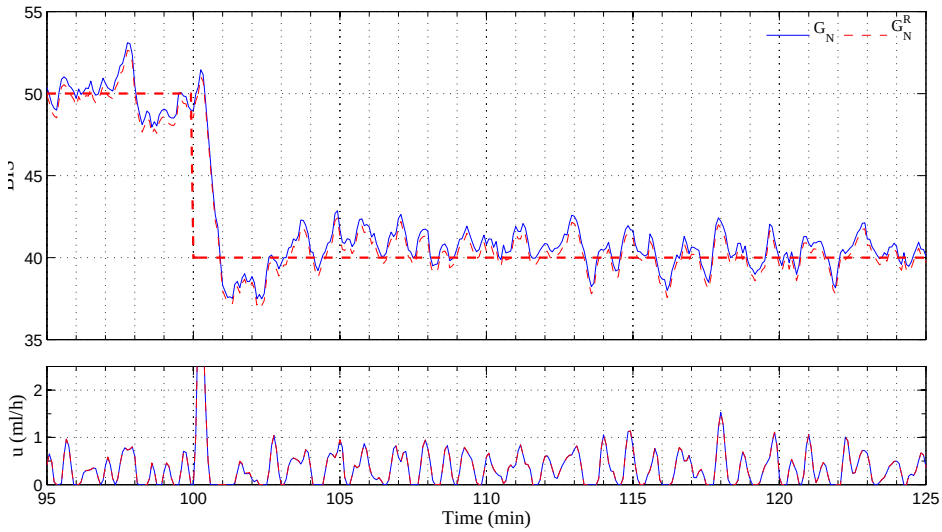

Figure 14. Time response of the controlled nominal model with the full order controller and the reduced-order controller (G_N^R). The reference is represented by the red dashed line.

reduced and discrete controller is presented in Fig. 15, and allows to conclude that the stability condition is still met for all the patient models.

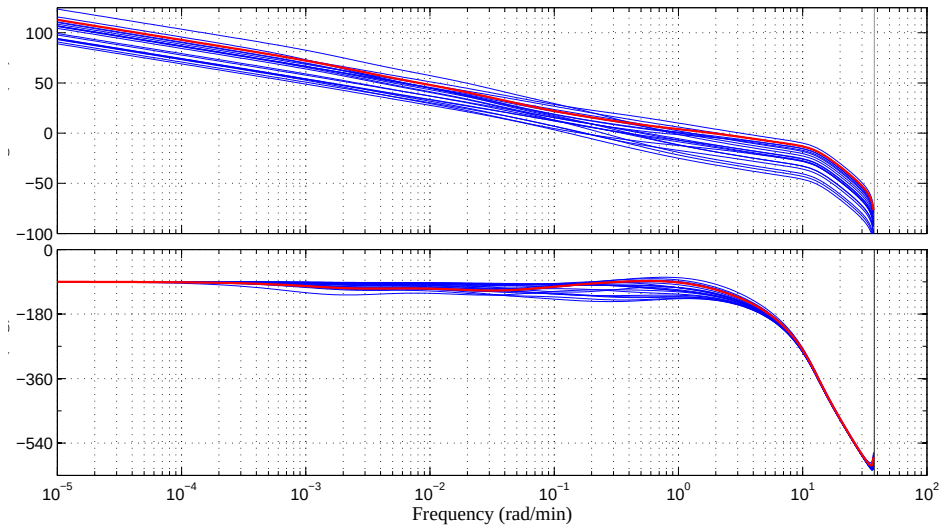

Figure 15. Loop-gain frequency response, with the discrete controller. The nominal model is represented in red.

Time response of a few models (G_1, G_2, G_4, G_8 and G_N) of the patient model bank with the discrete controller, of order 5, is presented in Fig. 16. This data shows that the controller is able to provide acceptable performances in time response with all models. Although models G_4 and G_{14} are excluded from the controller design, the controller presents a good performance when applied to these models, as is possible to see with the time response of model G_4, in Fig. 16.

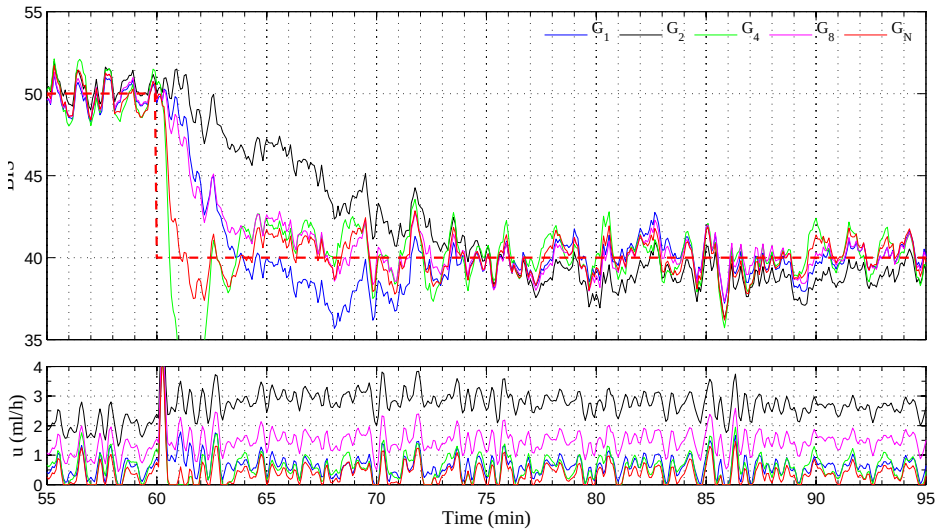

Figure 16. Time response of the controlled systems, with the discrete controller, and the control action for 5 models (G_1, G_2, G_4, G_8 and G_N). The reference is represented by the red dashed line.

5. Conclusions

An approach to the robust control of DoA based on H∞ design and μ-synthesis has been proposed and illustrated using a bank of patient model data. The approach consists in characterizing a multiplicative uncertainty model description for the patients, enlarging this model with an integrator to ensure zero steady-state tracking error, controller design using the DK-algorithm, controller order reduction, and controller redesign in discrete time to obtain a controller suitable to computer application.

The controller that is designed aiming at robust performance and stability is able to track the reference for all the models. The performance conditions are fulfilled for all the models except one for which its sensitivity function does not fall below the bound W_S^{-1}. This controller has robust stability for 18 of the 20 models, although the time responses for the two other models left out are considered clinically adequate. The fact that the bounds of performance are crossed is the cost for robust stability, that is the ultimate goal

to achieve at the problem at hand. The order reduction and the *a posteriori* discretization allows computer application with appropriate frequency and time responses.

References

[1] A.R. ABSALOM, N. SUTCLIFFE and G.N. KENNY: Closed-loop control of anesthesia using bispectral index: performance assessment in patients undergoing major orthopedic surgery under combined general and regional anesthesia. *Anesthesiology*, **96**(1), (2002), 67-73.

[2] S. ANNA and P. WEN: Depth of anesthesia control using internal model control techniques. In *2010 IEEE/ICME Int. Conf. on Complex Medical Engineering*, (2010), 294-300.

[3] G. BALAS, A. CHIANG, R. PACKARD and M. SAFANOV: *Robust Control Toolbox^{TM} User' Guide*. The MathWorks, Inc., 2012.

[4] T.W. BOUILLON, J. BRUHN, L. RADULESCU, C. ANDRESEN, T.J. SHAFER, C. CAROL and S.L. SHAFER: Pharmacodynamic interaction between propofol and remifentanil regarding hypnosis, tolerance of laryngoscopy, bispectral index, and electroencephalographic approximate entropy. *Anesthesiology*, **100**(6), (2004), 1353-1372.

[5] G.A. DUMONT, A. MARTINEZ and J.M. ANSERMINO: Robust control of depth of anesthesia. *Int. J. of Adaptive Control and Signal Processing*, **23**(5), (2009), 435-454.

[6] J.B. DYCK and S.L. SHAFTER: Effects of age on propofol pharmacokinetics. In *Seminars in Anesthesia*, **11** 2-4. Implemented in the computer program Stanpump, (1992).

[7] C.M. IONESCU, R. DE KEYSER, B.C. TORRICO, T. DE SMET, M.M. STRUYS and J.E. NORMEY-RICO: Robust predictive control strategy applied for propofol dosing using BIS as a controlled variable during anesthesia. *IEEE Trans. on Biomedical Engineering*, **55**(9), (2008), 2161-2170.

[8] L.A. KEARSE JR, C. ROSOW, A. ZASLAVSKY, P. CONNORS, M. DERSHWITZ and W. DENMAN: Bispectral analysis of the electroencephalogram predicts conscious processing of information during propofol sedation and hypnosis. *Anesthesiology*, **88**(1), (1998), 25-34.

[9] N. LIU, T. CHAZOT, A GENTY, A. LANDAIS, A. RESTOUX, K. MCGEE, P.A. LALOË, B. TRILLAT, L. BARVAIS and M. FISCHLER: Titration of propofol for anesthetic induction and maintenance guided by the bispectral index: closed-loop

versus manual control: a prospective, randomized, multicenter study. *Anesthesiology*, **104**(4), (2006), 686-695.

[10] B. MARSH, M. WHITE, N. MORTON and G.N.C. KENNY: Pharmacokinetic model driven infusion of propofol in children. *British J. of Anaesthesia*, **67**(1), (1991), 41-48.

[11] O. ORTOLANI, A. CONTI, A. DI FILIPPO, C. ADEMBRI, E. MORALDI, A. EVANGELISTI, M. MAGGINI and S.J. ROBERTS: EEG signal processing in anaesthesia. use of a neural network technique for monitoring depth of anaesthesia. *British J. of Anaesthesia*, **88**(5), (2002), 644-648.

[12] I.J. RAMPIL: A primer for EEG signal processing in anesthesia. *Anesthesiology*, **89**(4), (1998), 980-1002.

[13] T. SAKAI, A. MATSUKI, P.F. WHITE and A.H. GIESECKE: Use of an EEG-bispectral closed-loop delivery system for administering propofol. *Acta Anaesthesiologica Scandinavica*, **44**(8), (2000), 1007-1010.

[14] Y. SAWAGUCHI, E. FURUTANI, G. SHIRAKAMI, M. ARAKI and K. FUKUDA: A model-predictive hypnosis control system under total intravenous anesthesia. *IEEE Trans. on Biomedical Engineering*, **55**(3), (2008), 874-887.

[15] T.W. SCHNIDER, C.F. MINTO, P.L. GAMBUS, C. ANDRESEN, D.B. GOODALE, S.L. SHAFER and E.J. YOUNGS: The influence of method of administration and covariates on the pharmacokinetics and pharmacodynamics of propofol in adult volunteers. *Anesthesiology*, **88**(5), (1998), 1170-1182.

[16] J.S. SHIEH, D.A. LINKENS and A.J. ASBURY: A hierarchical system of on-line advisory for monitoring and controlling the depth of anaesthesia using self-organizing fuzzy logic. *Engineering Applications of Artificial Intelligence*, **18**(3), (2005), 307-316.

[17] S. SKOGESTAD and I. POSTLETHWAITE: *Multivariable Feedback Control Analysis and Design*. John Wiley & Sons, 2005.